

Molecular hydrogen in the disk of the Herbig Ae star HD 97048

C. Martin-Zaïdi¹, E. Habart², J.-C. Augereau¹, F. Ménard¹, P.-O. Lagage³, E. Pantin³ and
J. Olofsson¹

Received _____; accepted _____

¹Laboratoire d'Astrophysique de Grenoble, CNRS/UJF - UMR 5571, 414 rue de la Piscine, DU Saint Martin d'Hères, 38041 Grenoble cedex 9, France, claire.martin-zaidi@obs.ujf-grenoble.fr, augereau@obs.ujf-grenoble.fr, menard@obs.ujf-grenoble.fr, olofsson@obs.ujf-grenoble.fr

²Institut d'Astrophysique Spatiale, 91405 Orsay, France, emilie.habart@ias.u-psud.fr

³Laboratoire AIM, CEA/DSM - CNRS - Université Paris Diderot, DAPNIA/Service d'Astrophysique, Bat. 709, CEA/Saclay, 91191 Gif-sur-Yvette Cedex, France, pierre-olivier.lagage@cea.fr, epantin@cea.fr

ABSTRACT

We present high-resolution spectroscopic mid-infrared observations of the circumstellar disk around the Herbig Ae star HD 97048 obtained with the *VLT Imager and Spectrometer for the mid-InfraRed (VISIR)*. We conducted observations of mid-infrared pure rotational lines of molecular hydrogen (H_2) as a tracer of warm gas in the disk surface layers. In a previous paper, we reported the detection of the S(1) pure rotational line of H_2 at $17.035 \mu\text{m}$ and argued it is arising from the inner regions of the disk around the star. We used *VISIR* on the VLT for a more comprehensive study based on complementary observations of the other mid-infrared molecular transitions, namely S(2) and S(4) at $12.278 \mu\text{m}$ and $8.025 \mu\text{m}$ respectively, to investigate the physical properties of the molecular gas in the circumstellar disk around HD 97048. We do not detect neither the S(2) line nor the S(4) H_2 line from the disk of HD 97048, but we derive upper limits on the integrated line fluxes which allows us to estimate an upper limit on the gas excitation temperature, $T_{ex} < 570 \text{ K}$. This limit on the temperature is consistent with the assumptions previously used in the analysis of the S(1) line, and allows us to set stronger constraints on the mass of warm gas in the inner regions of the disk. Indeed, we estimate the mass of warm gas to be lower than $0.1 M_{\text{Jup}}$. We also discuss the probable physical mechanisms which could be responsible of the excitation of H_2 in the disk of HD 97048.

Subject headings: stars: pre-main sequence — stars: individual (HD97048) — (stars:) circumstellar matter — (stars:) planetary systems: protoplanetary disks — infrared: stars

1. Introduction

Disks around young stars are a natural outcome of the star formation process and the place for planet formation. At the present time, a significant effort has been done on the study of the dust in disks. However, the dust only represents a tiny fraction of the disk mass ($\sim 1\%$), and it is thus mandatory to deeply study the gas phase in disks in order to set stronger constraints on the giant planets formation process. Molecular hydrogen (H_2) is the most abundant molecule in the circumstellar (CS) environments of young stars and is supposed to be the key element of giant planet formation, thus its diagnostics are promising. Indeed, the detection of H_2 provides the most direct information about the gaseous content of disks, setting limits on the timescales for the dissipation of CS matter and possibly planet building. H_2 has been observed in CS environments at ultraviolet (e.g. Johns-Krull et al. 2000; Martin-Zaïdi et al. 2008) and near-infrared (e.g. Bary et al. 2003) wavelengths. These observations trace hot circumstellar gas, or gas excited by fluorescent processes, or require specific spatial distributions for the gas to be detectable. They are therefore difficult to translate into gas masses. The pure rotational mid-infrared H_2 lines are useful probes because the level populations are expected to be in local thermodynamic equilibrium (LTE) at the local gas temperature, and so line ratios allow determination of the excitation temperature and mass of the warm gas.

HD 97048 is a nearby, relatively isolated Herbig A0/B9 star, surrounded by a CS disk, located in the Chameleon cloud at a distance of 180 pc (van den Ancker et al. 1998). Its age has been estimated from evolutionary tracks to be of the order of 3 Myrs (kindly computed for us by L. Testi and A. Palacios). The *VISIR* (*VLT Imager and Spectrometer for the mid-InfraRed*; Lagage et al. 2004) imaging observations of this star have revealed emission of PAHs (Polycyclic Aromatic Hydrocarbons) at the surface of a flared disk extending at least up to 370 AU (Lagage et al. 2006). The flaring index has been measured to be

1.26 ± 0.05 , which is in good agreement with hydrostatic flared disk models (Lagage et al. 2006; Doucet et al. 2007). This is the only Herbig star for which the flaring of the disk has been observed by direct imaging. This geometry implies that a large amount of gas should be present to support the hydrostatic structure and that the disk is at an early stage of evolution. This star is thus one of the best candidates to study the gas component in the disks of HAes.

In a previous paper (Martin-Zaïdi et al. 2007, hereafter Paper I), we presented *VISIR* high-resolution spectroscopic mid-infrared observations of the circumstellar disk around the Herbig Ae (HAe) star HD 97048 near $17.03 \mu\text{m}$. Although Carmona et al. (2008) suggested, from their disk model with the assumptions of LTE conditions and gas-to dust ratio of about 100, that mid-IR H_2 lines should not be detected with the existing instruments, we detected the S(1) pure rotational line of molecular hydrogen at $17.035 \mu\text{m}$ arising from the disk around HD 97048. In addition, Bitner et al. (2007) have detected mid-IR H_2 rotational lines in the disk of another Herbig star, namely AB Aur, using the high spectral and spatial resolution TEXES spectrometer. These detections demonstrate that H_2 can be observed in the mid-IR domain when particular physical conditions exist in disks.

Despite the fact that the line is neither spatially nor spectrally resolved, the detection of the S(1) line in the disk of HD 97048 revealed the presence of significant amounts of warm gas in the inner 35 AU of the disk. Circumstellar gas had been previously detected in the disk of HD 97048 by Acke & van den Ancker (2006), who showed that the [O I] emission arises at radii between 0.5 and 60 AU from the central star. Very recently, modeling of near-infrared CO emission showed that the inner radius of the CO emitting region is located at 12 AU from the star (van der Plas et al. 2008). These observations reinforced the claim that the disk of HD 97048 contains large amounts of gas both at small and large radii, as suggested by the flaring geometry, and that HD 97048 is a young object surrounded by a

disk at an early stage of evolution. Indeed photoevaporation of the gas and planet formation clear up the inner part of the disk in timescales expected to be lower than 3 million years (Takeuchi et al. 2005; Gorti & Hollenbach 2008a,b). The H₂ S(1) line detection also implies that particular physical conditions for H₂ are present in the inner disk surface layer. The analysis of these data usually assumes that the H₂ excitation is in local thermodynamic equilibrium (LTE), and can itself thus be characterized by a single excitation temperature, which should be close to the gas temperature because of the low critical densities. As shown by the AB Aur observations (Bitner et al. 2007, 2008), the H₂ gas temperature could be significantly higher than the dust temperature in the disk surface layers of HD 97048, due to the dust settling or coagulation, for example. However, several competing mechanisms could contribute to the excitation of molecular hydrogen such as UV and X-rays heating, shocks, etc..., (see review papers by Habart et al. 2004; Snow & McCall 2006) and could be responsible for the observed emission. We refer the reader to Paper I for a complete discussion about the different possible explanations.

The detection of the other pure rotational lines of H₂ is a potentially powerful tool to determine the excitation temperature (and thus the mass) of the warm gas, and better constrain the excitation of H₂. In this paper, we thus present *VISIR* high-resolution spectroscopic observations of the two other pure rotational lines of H₂ observable from the ground: the S(2) line at 12.2786 μm , and the S(4) line at 8.0250 μm . We also recall the main results obtained from the S(1) line detection (detailed in Paper I).

2. Observations and data reduction

HD 97048 was observed at 3 different epochs. The observations at 17.035 μm presented in the Paper I were performed in 2006 June 22, the 8.025 μm observations in 2007 April 07, and the 12.278 μm observations in 2007 July 03. The three sets of observations were

obtained with the high-resolution spectroscopic mode of *VISIR*. The exposure time, slit width, and atmospheric conditions during the observations for the target star and standard references are presented in Table 1.

For all the three observations, the standard chopping and nodding technique was used to suppress the large sky and telescope background dominating at mid-IR wavelengths. Asteroids and standard stars were observed just before and after observing HD 97048, at nearly the same airmass and seeing conditions as the object. In order to correct the spectra from the Earth’s atmospheric absorption, we divided each spectrum of HD 97048 by that of the corresponding asteroid (which has a much better signal-to-noise ratio than that of the standard star), and used the standard stars observed and modeled spectra (Cohen et al. 1999) to obtain the absolute flux calibration. In order to verify our flux calibration, we checked the *Spitzer Space Telescope* archives. HD 97048 was observed with the IRS spectrograph installed onboard the *Spitzer Space Telescope* as part of the “Cores to Discs” (c2d) legacy program (AOR:0005644800, PI: Evans). The data reduction was performed using the *c2d* legacy team pipeline (Lahuis et al. 2006) with the S15.3.0 pre-reduced (BCD) data. The absolute flux calibration of our *VISIR* data in the 3 wavelength ranges has been performed in order to be consistent with the *Spitzer* flux measurements. We estimate the error on the absolute flux calibration to be lower than 10% , a value which does not affect our analysis.

The wavelength calibration is done by fitting the observed sky background features with a model of Paranal’s atmospheric emission (for more details on the observation and data reduction techniques see Paper I). We note that $A_v = 0.24$ mag for HD 97048 (Valenti et al. 2000), thus we have not corrected the spectra for dust extinction, since it is negligible in our wavelength range for any $A_v < 40$ mag (Fluks et al. 1994).

3. Results

3.1. Non-detection of the S(2) and S(4) lines

HD 97048 spectra show no evidence for H₂ emission neither at 12.278 μm nor at 8.025 μm (Fig. 1, middle and bottom panels). For each flux-calibrated spectrum, we calculated the standard deviation (σ) for wavelength ranges relatively unaffected by telluric absorption, and close to the wavelength of interest. The 3σ upper limits on the integrated line fluxes were calculated by integrating over a Gaussian of FWHM equal to a spectral resolution element (21 km s⁻¹) and an amplitude of about 3σ flux (Fig. 1). We assumed the same radial velocity for the S(2) and S(4) lines than that observed for the S(1) line and corrected appropriately for each epoch of observation. We thus centered the Gaussian on the expected wavelengths for the S(2) and S(4) lines respectively (see Table 2). From the limits on integrated intensities, we estimated the upper limits on the column densities of the corresponding upper rotational levels of each H₂ transition (see Table 2). For this purpose, we first assumed that the line is optically thin and that the radiation is isotropic. In this context, the column densities are derived from the following formula (van Dishoeck 1992):

$$I_{ul} = \frac{hc}{4\pi\lambda} N_u(H_2) A_{ul} \quad \text{ergs s}^{-1} \text{cm}^{-2} \text{sr}^{-1}, \quad (1)$$

where I_{ul} is the integrated intensity of the line, λ is the wavelength of the transition $J = u - l$, A_{ul} is the spontaneous transition probability, $N_u(H_2)$ is the column density of the upper rotational level of the transition.

3.2. Detection of the S(1) line at 17.035 μm

We recall here the results of our analysis of the S(1) line. For more details, we refer the reader to the Paper I. As shown in Fig. 1 (top panel), we have detected the H_2 pure rotational S(1) line near 17.03 μm . In the flux-calibrated spectrum, the standard deviation (σ) of the continuum flux was calculated in regions less influenced by telluric absorption, and close to the feature of interest. We deduced a 6σ detection in amplitude for the line, corresponding to a signal-to-noise ratio of about 11σ for the line, when integrating the signal over a resolution element (6 pixels). The line is not spectrally resolved as we can fit it with a Gaussian with a full width at half maximum (FWHM) equal to a spectral resolution element of 21 km s^{-1} (Fig. 1). From our fit, we derived the integrated flux in the line (see Table 2). Once the spectrum is corrected from the Earth’s rotation, and knowing the heliocentric radial velocity of HD 97048 ($+21 \text{ km s}^{-1}$; Acke et al. 2005), we estimated, from the wavelength position of the Gaussian peak, the radial velocity of H_2 to be about $4\pm 2 \text{ km s}^{-1}$ in the star’s rest frame. We thus considered that the radial velocity of the H_2 is compatible with zero (at the *VISIR* resolution) and therefore similar to that of the star, implying that the emitting gas is gravitationally bound to the star, and likely arising from the disk and not from an outflow. H_2 outflows from T Tauri stars usually have (blueshifted) velocities of a few tens up to a hundred of km s^{-1} when a clear outflow is identified. Otherwise, when the line is detected at zero systemic velocity and is narrow or unresolved as is the case here, it is generally attributed to the disk (e.g. Herczeg et al. 2006; Bitner et al. 2008). The H_2 line is not resolved spatially either. Given the *VISIR* spatial resolution of about $0.427''$ at 17.03 μm , and the star distance (180 pc from the Sun), we can assess that the emitting H_2 is located within the inner 35 AU of the disk. Assuming that the H_2 gas follows the same (Keplerian) kinematics as the disk, the emitting gas observed with *VISIR* is likely not concentrated significantly in the innermost AU of the disk ($< 5 \text{ AU}$) otherwise rotational broadening would be observed. Indeed, near the

central star, the rotational velocity of the disk is of the order of a hundred of km s^{-1} , to be compared to the spectral resolution of VISIR, 21 km s^{-1} . The emitting H_2 is thus more likely distributed in an extended region within the inner disk, between 5 AU and 35 AU of the disk. Assuming the emission arises from an isothermal mass of optically thin H_2 , we estimated the corresponding column densities and masses of H_2 as a function of prescribed temperatures (for 150 K, 300 K and 1000 K; see Paper I for details about the method). In Table 2 are reported the integrated flux of the S(1) line, its intensity, and the corresponding column density for the $J = 3$ rotational level. Since we have a signal-to-noise ratio of about 11σ for the line, we can deduce 9% error bars on these values (see Table 2).

3.3. Physical properties of H_2

The estimates of the column densities of the $J = 3$, $J = 4$, and $J = 6$ rotational levels of H_2 allowed us to plot the excitation diagram of H_2 (see Fig. 2). Assuming that all three levels are populated by thermal collisions (LTE), we estimated the excitation temperature of the observed gas. The upper limit on the column density of the $J = 6$ level strongly constrains the value of the column density of the $J = 4$ level. Indeed, the population of the $J = 4$ level should correspond to the excitation temperature given by the ratio of the column densities of the $J = 3$ and $J = 6$ levels. We assumed that the population of the $J = 3$ and $J = 6$ levels follow the Boltzmann law, which corresponds to a linear fit to the points on the excitation diagram (Fig. 2):

$$\frac{N(\text{H}_2)_{J=3}}{N(\text{H}_2)_{J=6}} = \frac{g_3}{g_6} \times \exp\left(-\frac{E_3 - E_6}{k T_{ex}}\right), \quad (2)$$

where $N(\text{H}_2)_{J=i}$ is the column density, g_i is the statistical weight, and E_i is the energy of the $J = i$ level; k is the Boltzmann constant and T_{ex} is the temperature defined as the

excitation temperature. Since we only have upper limits on the column densities of the $J = 4$ and $J = 6$ levels, only an upper limit on the excitation temperature is relevant. Since the temperature is inversely proportional to the slope on the excitation diagram, in order to obtain the upper limit on the excitation temperature, we considered the lower value of the column density of the $J = 3$ level (i.e., the measured value minus 1σ) and the upper limit on the $J = 6$ population level (that procedure yields the minimum slope / maximum temperature and corresponds to the solid line on Fig. 2). We thus find that the excitation temperature of H_2 should be lower than 570 K. In this case, the column density of the $J = 4$ level should be lower than $1.6 \times 10^{20} \text{ cm}^{-2}$ which is lower than the value obtained from the 3σ upper limit (see Table 2).

Under the assumption that the H_2 emission is optically thin, that the emitting H_2 is in LTE at a temperature of about 570 K, and that the source size is equal or smaller than *VISIR*'s beam size, we derived upper limits on the H_2 mass (see Table 2):

$$M_{gas} = f \times 1.76 \times 10^{-20} \frac{F_{ul} d^2}{(hc/4\pi\lambda) A_{ul} x_u(T)} M_{\odot} , \quad (3)$$

where F_{ul} is the line flux, d the distance in pc to the star, $x_u(T)$ is the fractional population of the level u at the temperature T in LTE (for details on the calculation method, see van Dishoeck 1992), f is the conversion factor required for deriving the total H_2 gas mass from the H_2 -ortho or H_2 -para mass. Since $M_{H_2} = M_{H_2}(\text{ortho}) + M_{H_2}(\text{para})$, then $f = 1 + 1/(\text{ortho}/\text{para})$ for the S(1) line (a H_2 -ortho transition) and $f = 1 + \text{ortho}/\text{para}$ for the S(2) and S(4) lines (H_2 -para transitions). The equilibrium ortho-para ratio at the temperature T was computed using Eq.(1) from Takahashi (2001).

4. Discussion

Our previous high-resolution spectroscopic observations with *VISIR* of the S(1) pure rotational line of H₂ at 17.035 μm of HD 97048 revealed the presence of significant amounts of warm gas in the surface layer of the disk in the inner 35 AU from the central star (Paper I). This detection confirmed that HD 97048 is a young object surrounded by a circumstellar disk at an early stage of evolution, still rich in gas.

In the present paper, we report the non-detections of the S(2) and S(4) lines of H₂ in the disk of the Herbig Ae star HD 97048. Using *VISIR* high-resolution spectra, we compute upper limits for the column densities of the $J = 4$ and $J = 6$ rotational levels. Using the results obtained from the analysis of the S(1) line (column density of the $J = 3$ level), and assuming that the $J = 3$ to $J = 6$ levels are excited by thermal collisions we derive an upper limit on the excitation temperature of H₂ of about 570 K.

This constraint on a temperature lower than 570 K for the gas allows us to set a stronger constraint on the mass of warm H₂ ($< 0.1 M_{\text{Jup}}$; $1 M_{\text{Jup}} \sim 10^{-3} M_{\odot}$) in the inner 35 AU of the disk than that estimated in Paper I. Indeed, in Paper I, we derived masses of the warm gas in the range from 10^{-2} to nearly $1 M_{\text{Jup}}$, for temperatures in the range from 150 K to 1000 K and assuming LTE. The mass of warm gas we estimate is also lower than that we derived from the paper by Lagage et al. (2006) who estimated the mass of H₂ in the disk to be of about $0.01 M_{\odot}$. By assuming that the surface density Σ follows a power law $\Sigma(r) = \Sigma(r/370)^q$ with an index q equal to $-3/2$ (Lagage et al. 2006), we estimated in Paper I a minimum mass of gas in the inner 35 AU of the disk to be of the order of $3 M_{\text{Jup}}$. But it should be pointed out that mid-IR H₂ lines are only probing warm gas located in the surface layer of the disk, when a higher mass of colder gas is expected to be present in the interior layers of the disk.

However, from their disk model, Carmona et al. (2008) concluded that the expected

peak flux of the S(1) line at $17.035 \mu\text{m}$, observed at a spectral resolution of 20 000, should be less than 0.3% of that of the continuum at temperatures higher than 150 K, and thus should not be observable with the existing instruments. Those authors used a two-layer model (Chiang & Goldreich 1997; Dullemond et al. 2001) of a gas-rich disk (column density of $N(\text{H}_2)=10^{23} \text{ cm}^{-2}$) seen face-on, located at 140 pc from the Sun, with LTE for the gas and dust, $T_{gas}=T_{dust}$, and assumed a constant gas-to-dust mass ratio about 100.

As shown in Paper I from the observation of the S(1) line in the disk of HD 97048, such a detection can only be explained if the physical conditions of the gas differ from those used by Carmona et al. (2008). In Paper I, we proposed several ways to explain our detection. First, assuming equal dust and gas temperatures (LTE), we estimated gas-to-dust mass ratios much larger than the canonical value of 100. This hypothesis can not be ruled out by the non-detections of the S(2) and S(4) lines. One possible interpretation to explain a very high gas-to-dust ratio is that the dust is partially depleted from the uppermost disk surface layer, where the H_2 emission originates. The spatial decoupling between the gas and the dust may be due to low densities in the surface layers, or dust settling and coagulation into larger particles. The physical conditions may thus rapidly differ from the LTE ones, i.e. $T_{gas} > T_{dust}$. In the upper disk surface layers, photoelectric heating can thus play a significant role in the gas heating process (Kamp & Dullemond 2004; Jonkheid et al. 2007). In addition, photoelectric heating will be much efficient on small grains, such as PAHs, which show significant features in the different observations of HD 97048 (e.g. Doucet et al. 2007, and reference therein). Our upper limit on the excitation temperature is consistent with photoelectric heating. Indeed, as shown by Kamp & Dullemond (2004), photoelectric heating is characterized by a temperature limit (~ 1000 K) since for high stellar UV flux, grain ionization can be so large that the photoelectric effect is less efficient and T_{gas} does not increase anymore.

However, our observations do not allow us to rule out the possibility of a gas heating due to other excitation mechanisms such as UV pumping or X-ray heating. Indeed, UV and X-ray heating are likely possibilities that can heat the gas to temperatures significantly hotter than the dust. Nomura & Millar (2005) modeled UV heating of circumstellar disks around T Tauri stars and the resulting H₂ emission. In their model the temperature can be of about 1000 K at 10 AU from the central star, and the predicted H₂ S(2) line flux is about 2×10^{-15} ergs s⁻¹ cm⁻². This value is lower than our upper limit on the S(2) line flux, but their model was for a less massive star and disk.

The upper limit on the excitation temperature of about 570 K we found for H₂ in the disk of HD 97048, could also be consistent with X-ray heating. Very recently, Ercolano et al. (2008) demonstrated from their two-dimensional photoionization and dust radiative transfer models of a disk irradiated by X-rays from a T Tauri star, that the uppermost layers of gas in the disk could reach temperatures of 10⁶ K at small radii (<0.1 AU) and 10⁴ K at a distance of 1 AU. The gas temperatures decrease sharply with depth, but appear to be completely decoupled from dust temperatures down to a column depth of $\sim 5 \times 10^{21}$ cm⁻². These results are consistent with those of Glassgold et al. (2007) who computed that at 20 AU from the central star, the temperature can reach 3000 K at the surface of the disk before dropping to 500-2000 K in a transition zone and then to much cooler temperatures deep in the disk. By extrapolation, these models suggest that in the inner 35 AU from the central star, the upper layers of the disk could reach temperatures consistent with the upper limit of about 570 K we find for HD 97048.

The kinetic temperature of the gas is generally supposed to be given by the population of the first rotational levels (namely $J = 0$ and $J = 1$) since their critical densities are relatively low, and can not be higher than the excitation temperature given by the higher energy levels. Thus, in any case, even if the H₂ we observe around HD 97048 is not

essentially excited by thermal collisions, the populations of the three levels derived from our observations give strong constraints on the gas kinetic temperature. Our upper limit on the temperature of about 570 K is thus reliable whatever the mechanisms responsible for the excitation of the observed gas. We stress that the excitation temperature we find for H₂ from the *VISIR* observations of HD 97048 is close to that derived from the TEXES observations of AB Aur (670 K) by Bitner et al. (2007), which reinforces the similarities between the two stars (see Paper I).

In order to better constrain the physical conditions of H₂, high-sensitivity and high-resolution space-based spectrographs in the mid-IR would be required (e.g. Boulanger et al. 2008). In particular, only the observation of the S(0) emission line near 28 μ m would allow us to clearly constrain both the kinetic temperature of the observed gas and the physical mechanisms responsible its excitation.

This work is based on observations obtained at ESO/VLT (Paranal) with *VISIR*, programs' number 079.C-0839A and 079.C-0839B. CMZ is supported by a CNES fellowship. This work was supported by *Agence Nationale de la Recherche* (ANR) of France through contract ANR-07-BLAN-0221. We also thank *Programme National de Physique Stellaire* (PNPS) of CNRS/INSU, France, for supporting part of this research.

Facilities: ESO/VLT VISIR

REFERENCES

- Acke, B. & van den Ancker, M. E. 2006, *A&A*, 449, 267
- Acke, B., van den Ancker, M. E., & Dullemond, C. P. 2005, *A&A*, 436, 209
- Bary, J. S., Weintraub, D. A., & Kastner, J. H. 2003, *ApJ*, 586, 1136
- Bitner, M. A., Richter, M. J., Lacy, J. H., et al. 2008, *ApJ*, 688, 1326
- Bitner, M. A., Richter, M. J., Lacy, J. H., et al. 2007, *ApJ*, 661, L69
- Boulanger, F., Maillard, J. P., Appleton, P., et al. 2008, *Experimental Astronomy*, 20+-
- Carmona, A., van den Ancker, M. E., Henning, T., et al. 2008, *A&A*, 477, 839
- Chiang, E. I. & Goldreich, P. 1997, *ApJ*, 490, 368
- Cohen, M., Walker, R. G., & Witteborn, F. C. 1999, *LPI Contributions*, 969, 5
- Doucet, C., Habart, E., Pantin, E., et al. 2007, *A&A*, 470, 625
- Dullemond, C. P., Dominik, C., & Natta, A. 2001, *ApJ*, 560, 957
- Ercolano, B., Drake, J. J., Raymond, J. C., & Clarke, C. C. 2008, *ApJ*, 688, 398
- Fluks, M. A., Plez, B., The, P. S., et al. 1994, *A&AS*, 105, 311
- Glassgold, A. E., Najita, J. R., & Igea, J. 2007, *ApJ*, 656, 515
- Gorti, U. & Hollenbach, D. 2008a, *ApJ*, 683, 287
- Gorti, U. & Hollenbach, D. 2008b, *ArXiv e-prints*
- Habart, E., Boulanger, F., Verstraete, L., Walmsley, C. M., & Pineau des Forêts, G. 2004, *A&A*, 414, 531

- Herczeg, G. J., Linsky, J. L., Walter, F. M., Gahm, G. F., & Johns-Krull, C. M. 2006, *ApJS*, 165, 256
- Johns-Krull, C. M., Valenti, J. A., & Linsky, J. L. 2000, *ApJ*, 539, 815
- Jonkheid, B., Dullemond, C. P., Hogerheijde, M. R., & van Dishoeck, E. F. 2007, *A&A*, 463, 203
- Kamp, I. & Dullemond, C. P. 2004, *ApJ*, 615, 991
- Lagage, P.-O., Doucet, C., Pantin, E., et al. 2006, *Science*, 314, 621
- Lagage, P. O., Pel, J. W., Authier, M., et al. 2004, *The Messenger*, 117, 12
- Lahuis, F., Kessler-Silacci, J. E., Evans, N. J., I., et al. 2006, *c2d Spectroscopy Explanatory Supplement*, Tech. rep., Pasadena: Spitzer Science Center
- Martin-Zaïdi, C., Deleuil, M., Le Bourlot, J., et al. 2008, *A&A*, 484, 225
- Martin-Zaïdi, C., Lagage, P.-O., Pantin, E., & Habart, E. 2007, *ApJ*, 666, L117
- Nomura, H. & Millar, T. J. 2005, *A&A*, 438, 923
- Snow, T. P. & McCall, B. J. 2006, *ARA&A*, 44, 367
- Takahashi, J. 2001, *ApJ*, 561, 254
- Takeuchi, T., Clarke, C. J., & Lin, D. N. C. 2005, *ApJ*, 627, 286
- Valenti, J. A., Johns-Krull, C. M., & Linsky, J. L. 2000, *ApJS*, 129, 399
- van den Ancker, M. E., de Winter, D., & Tjin A Djie, H. R. E. 1998, *A&A*, 330, 145
- van der Plas, G., van den Ancker, M. E., Acke, B., et al. 2008, *ArXiv e-prints*

van Dishoeck. 1992, in *Infrared Astronomy with ISO*, ed. Encrenaz, Th., and Kessler, M.F. (Nova Science Publisher), 283

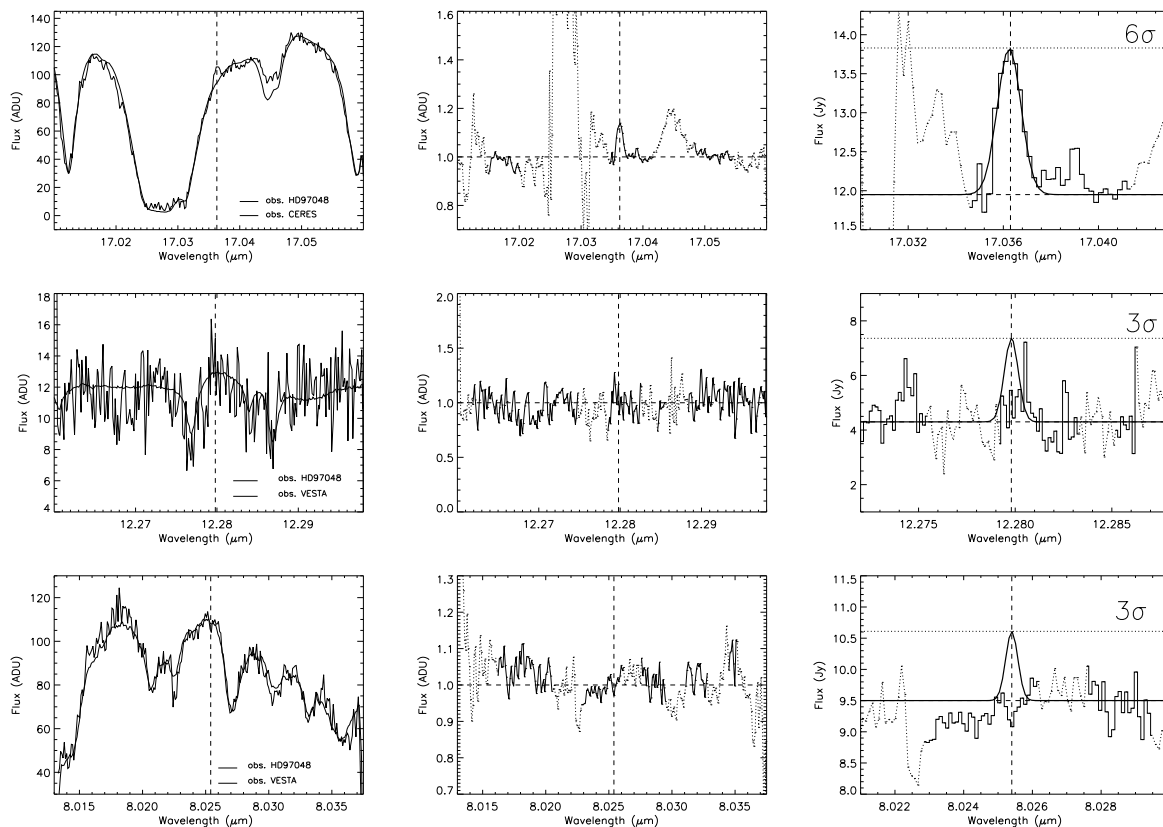


Fig. 1.— *VISIR* spectra of HD 97048 at 17.035 μm (*top panel*), 12.278 μm (*middle panel*) and 8.025 μm (*bottom panel*). *Left panel*: continuum spectra of the asteroid and of the target before telluric correction. *Central panel*: full corrected spectra: dotted lines show spectral regions strongly affected by telluric features. *Right panel*: zoom of the region where the H_2 lines should be observed (dashed vertical lines). The spectra were corrected neither for the radial velocity of the targets nor the Earth’s rotation velocity.

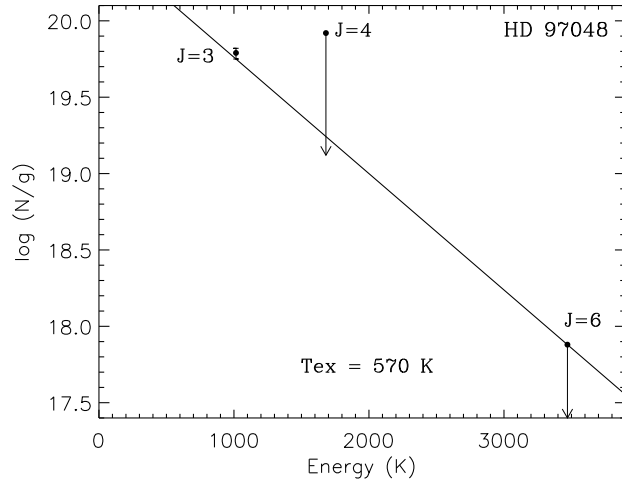


Fig. 2.— Excitation diagram for H₂ towards HD 97048. If the three rotational levels are populated by thermal collisions, their populations follow the Boltzmann law, and the upper limit on the excitation temperature is given by considering the lower limit on the column density of the $J = 3$ level and the upper limit on the $J = 6$ population level (solid line). Thus, in this case, the gas temperature should be lower than 570 K.

Table 1: Summary of the observations. The airmass and seeing intervals are given from the beginning to the end of the observations.

λ (μm)	t_{exp} (s)	Airmass	Optical seeing (")	Slit (")	R	Stand. Star	Airmass	Optical seeing (")	Asteroid	Airmass	Optical seeing (")
17.0348	1800	1.72-1.79	0.52-0.66	0.75	14 000	HD89388	1.90-1.94	0.60-0.72	CERES	1.68-1.82	0.58-0.69
12.2786	960	1.81-1.87	1.97-2.16	0.4	13 600	HD91056	1.82-1.87	1.39-1.82	VESTA	1.03-1.04	1.67-2.23
8.0250	1872	1.66-1.69	0.51-0.65	0.4	13 300	HD92305	1.69-1.70	0.64-0.65	VESTA	1.54-1.59	0.75-0.79

Table 2: Fluxes, intensities, luminosities and column densities of each observed mid-IR transitions of H_2 . The mass of H_2 is calculated for a temperature of about 570 K. λ_{obs} is the wavelength of the centroid of the line. v_{up} and J_{up} are respectively the vibrational and rotational upper levels of the transition of interest.

λ_{obs} (μm)	Transition	v_{up}	J_{up}	Continuum flux ^a (Jy)	Integrated line flux ($\text{ergs s}^{-1} \text{cm}^{-2}$)	Line intensity ($\text{ergs cm}^{-2} \text{s}^{-1} \text{sr}^{-1}$)	Line luminosity $\log(L/L_{\odot})$	$N_{J_{up}}(\text{H}_2)$ (cm^{-2})	$M(\text{H}_2)$ (M_{Jup})
17.03625	S(1)	0	3	11.95 ± 0.94	$2.4 \pm 0.2 \times 10^{-14}$	$5.7 \pm 0.5 \times 10^{-3}$	-4.61 ± 0.04	$1.29 \pm 0.12 \times 10^{21}$	$1.6 \pm 0.1 \times 10^{-2}$
12.2798	S(2)	0	4	4.3 ± 3.0	$< 5.5 \times 10^{-14}$	$< 2.6 \times 10^{-2}$	< -4.25	$< 7.46 \times 10^{20}$	$< 1.0 \times 10^{-1}$
8.0254	S(4)	0	6	9.5 ± 1.1	$< 4.7 \times 10^{-15}$	$< 5.1 \times 10^{-3}$	< -5.32	$< 9.80 \times 10^{18}$	$< 1.0 \times 10^{-2}$

^a: The error bars on the continuum fluxes are 3σ error bars.